

**Spin waves in permalloy nanowires: The importance of easy-plane anisotropy**

T. M. Nguyen and M. G. Cottam\*

*Department of Physics and Astronomy, University of Western Ontario, London, Ontario, Canada N6A 3K7*

H. Y. Liu, Z. K. Wang, S. C. Ng, and M. H. Kuok

*Department of Physics, National University of Singapore, Singapore 117542, Singapore*

D. J. Lockwood

*Institute for Microstructural Sciences, National Research Council, Ottawa, Canada K1A 0R6*

K. Nielsch and U. Gösele

*Max-Planck Institute of Microstructure Physics, Weinberg 2, D-06120 Halle, Germany*

(Received 3 January 2006; published 11 April 2006)

Brillouin light scattering has been employed to study the magnetic-field dependence of the discrete spin waves in permalloy  $\text{Ni}_{80}\text{Fe}_{20}$  nanowires. When a small magnetic field is applied transverse to the nanowire, the results reveal a low-frequency mode, which is absent in the longitudinal case. A Hamiltonian-based microscopic theory for nanowires with inhomogeneous magnetization shows that the appearance of this mode, along with its higher-field behavior, is a significant consequence of a small easy-plane single-ion anisotropy at the nanowire surface. The calculations provide a good description of experimental data for both the transverse and longitudinal cases.

DOI: [10.1103/PhysRevB.73.140402](https://doi.org/10.1103/PhysRevB.73.140402)

PACS number(s): 75.30.Ds, 75.30.Gw, 75.75.+a, 78.35.+c

The general dynamical properties of magnetic nanostructures such as arrays of dots, rings, and wires, are of great interest in both basic science and technological applications, e.g., in magnetic recording and sensor devices.<sup>1,2</sup> The study of spin waves (SWs) in these systems is of fundamental importance for understanding the magnetic interactions, while from a technological perspective the SWs define the time scale for the dynamics of the magnetization in switching processes. Investigation of the quantized SW modes by Brillouin light scattering (BLS) can be useful in probing many properties of these systems such as exchange stiffness, anisotropy terms, dipolar coupling between elements, inhomogeneity of the internal field, etc.<sup>3–10</sup> Other experiments on the SWs in spatially confined magnets have utilized ferromagnetic resonance (FMR) (Ref. 11) and time-resolved Kerr microscopy.<sup>12</sup>

BLS was successfully employed in earlier work<sup>8</sup> to study the SW quantization in ferromagnetic nickel nanowires. The authors showed that a preliminary interpretation using macroscopic theory<sup>13</sup> was satisfactory for the zero applied magnetic-field results, but the experimental data in a transverse field have only recently been explained using a microscopic (or Hamiltonian-based) model that allows for inhomogeneous magnetization.<sup>14,15</sup> In another theoretical work,<sup>16</sup> the SW frequencies in the transverse-field case have been calculated within the framework of a macroscopic approach by assuming that the magnetization remains uniform but canted away from the symmetry axis. Although the results in Ref. 16 explain qualitatively the experimental data of Ref. 8, the assumption of uniform magnetization represents a limitation when the applied field is comparable with the switching field for the magnetization direction and/or there is a surface anisotropy.

The BLS data reported here for arrays of permalloy

( $\text{Ni}_{80}\text{Fe}_{20}$ ) nanowires show features that are distinct compared to the nickel case. In particular, in the case of a small transverse applied field we observe a low-frequency branch in the SW spectrum that is absent in the longitudinal-field studies for permalloy nanowires<sup>10</sup> and that also has no counterpart in the corresponding measurement for nickel.<sup>8</sup> As the magnitude of the transverse field is increased, a SW hybridization (or mixing) effect is seen for permalloy in the vicinity of the switching field. These data have necessitated an extension of the microscopic theory to include various possibilities for single-ion anisotropy, as we discuss here, and are indicative of nonuniform magnetization being more significant than in the nickel case.

In the fabrication of the two-dimensional (2D) arrays of cylindrical nanowires, templates were first prepared from aluminum substrates based on a two-step electrochemical anodization process.<sup>17</sup> The nanowire arrays were then synthesized by filling the resulting hexagonally ordered porous  $\text{Al}_2\text{O}_3$  templates with  $\text{Ni}_{80}\text{Fe}_{20}$  by means of pulsed electrodeposition. Scanning electron microscope measurements showed that the permalloy nanowires have a wire diameter of 35 nm, a length of about 1  $\mu\text{m}$ , and a periodic wire spacing of 105 nm.

The Brillouin measurements were performed at room temperature in the  $180^\circ$ -backscattering geometry using a (3+3)-pass tandem Fabry–Perot interferometer equipped with a silicon avalanche diode detector, and 100 mW of the 514.5-nm radiation of an argon ion laser. A continuous stream of pure argon gas was directed at the irradiated spot on the sample surface to cool it and to keep air away from it. The applied magnetic field used was generated by a computer controlled 1.2 T electromagnet. For the transverse and longitudinal magnetic-field measurements, the symmetry axes of the nanowires were, respectively, aligned perpendicular

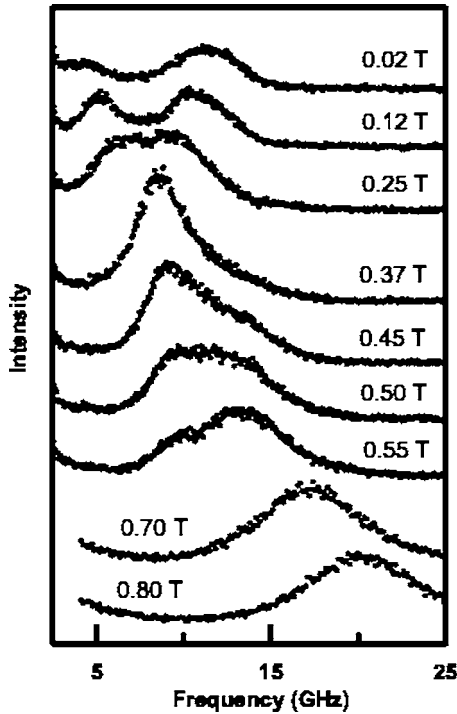


FIG. 1. Brillouin Stokes spectra from an array of  $\text{Ni}_{80}\text{Fe}_{20}$  nanowires at room temperature for various values of the transverse magnetic field.

and parallel to the magnetic field. All spectra were recorded in the  $p$ - $s$  polarization. Figure 1 shows several BLS spectra, each of which in general features two magnon peaks, of the  $\text{Ni}_{80}\text{Fe}_{20}$  nanowire sample recorded at various transverse magnetic fields. A crossing (or anticrossing) of the two SW peaks is evident in Fig. 1. Spectra recorded in the longitudinal field orientation also each contain two magnon peaks,<sup>10</sup> but in this case the peaks are well separated. The spectral peaks were fitted with a Lorentzian function, and the variations of the fitted SW frequencies with transverse and longitudinal magnetic fields are displayed in Figs. 2 and 3, respectively.

The theoretical calculations here are based on a model that was developed in a previous paper<sup>14</sup> and later extended to apply to the nickel nanowires.<sup>15</sup> Briefly, a single nanowire is modeled as having a macroscopically large number of layers of spins stacked vertically above each other (with spacing  $a$ ) along the  $y$  axis from  $-\infty$  to  $\infty$ . Previously<sup>14,15</sup> each cross-section layer (in the  $xz$  plane) was approximated as a hexagon with radius  $R=ra$ , and the spins were arranged on a triangular lattice (also with lattice constant  $a$ ). The total number of spins  $N$  in each layer is  $3r(r+1)+1$  for  $r=0,1,2,\dots$ . In this communication, for a more detailed comparison, we have also considered each cross-section layer in the nanowire to have  $N$  spins arranged on a square lattice but confined within a circle of radius  $R$ . In fact, for a sufficiently small value of  $a$ , and hence large value of  $N(>300)$ , the two alternative models are found to give very similar results as we discuss later. A nanowire can be described by the spin Hamiltonian

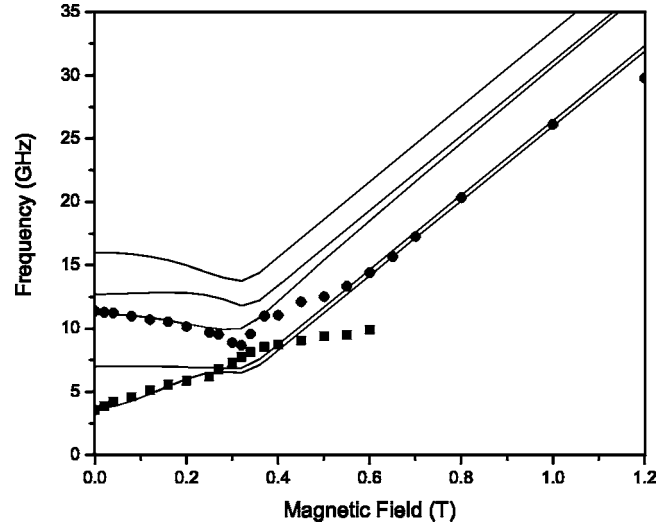


FIG. 2. Dependence of the SW frequencies on the applied magnetic field in the transverse case. Data points for the lowest two branches are indicated by the squares and circles. The lowest few theory curves are shown by the solid lines.

$$H = -\frac{1}{2} \sum_{in,jm} V_{in,jm}^{\alpha\beta} S_{in}^{\alpha} S_{jm}^{\beta} - g\mu_B \sum_{in} \mathbf{H}_0 \cdot \mathbf{S}_{in} - \sum_{in} K_n (S_{in}^y)^2. \quad (1)$$

Here  $i$  and  $j$  are indices for the individual layers,  $n$  and  $m$  label the position of the spins in a particular layer, and  $\alpha$  and  $\beta$  denote Cartesian components  $x$ ,  $y$ , or  $z$ . The coupling tensor  $V_{in,jm}$  between the two spins  $\mathbf{S}_{in}$  and  $\mathbf{S}_{jm}$  includes both the dipole-dipole and exchange interactions, and is given by

$$V_{in,jm}^{\alpha\beta} = -(g\mu_B)^2 \frac{|\mathbf{r}_{in,jm}|^2 \delta_{\alpha\beta} - 3r_{in,jm}^{\alpha} r_{in,jm}^{\beta}}{|\mathbf{r}_{in,jm}|^5} + J_{in,jm} \delta_{\alpha\beta}, \quad (2)$$

where  $\mathbf{r}_{in,jm} = (x_m - x_n, y_j - y_i, z_m - z_n)$ , and the equal-site case ( $i=j, n=m$ ) is excluded from the sum in Eq. (1). The ex-

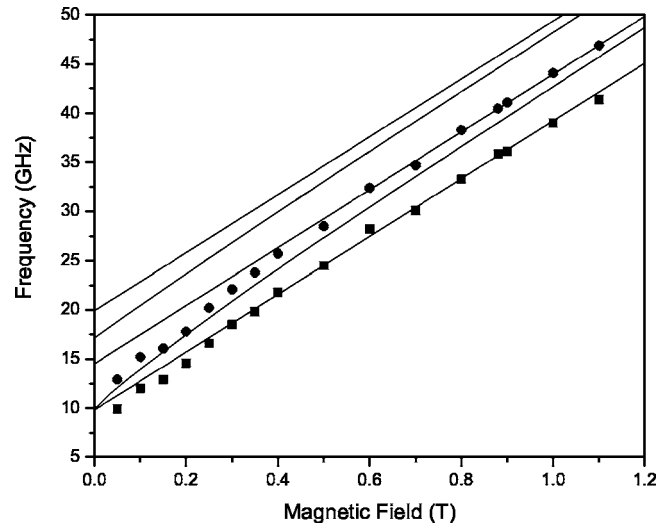


FIG. 3. Same as in Fig. 2 but for the longitudinal case.

change  $J_{in,jm}$  between the spins at sites  $r_{in}$  and  $r_{jm}$  is taken to be  $J$  (or  $J_{\perp}$ ) between nearest neighbors along the  $y$  axis (or in the  $xz$  plane), and zero otherwise. The second term in Eq. (1) represents the Zeeman energy due to an external magnetic field which is chosen to be in the  $yz$  plane, so  $\mathbf{H}_0 = (0, H_{\parallel}, H_{\perp})$  in general.

As an extension of the previous theory,<sup>14,15</sup> the final term in Eq. (1) allows for the inclusion of single-ion anisotropy, which can be either of the “easy-axis” type ( $K_n > 0$ ) or the “easy-plane” type ( $K_n < 0$ ). Also the coefficient  $K_n$  may be site dependent, and in particular it may be different at a surface site compared to the bulk. In general, the magnetization of the nanowire is inhomogeneous, and the equilibrium configuration of the spins needs to be found by minimizing the classical ground-state energy of the system. This can be done for any chosen set of parameter values by an iteration procedure as follows. As a starting approximation, we set the anisotropy to be zero and find the equilibrium configuration by the method used in Ref. 14. Starting from this configuration but with the anisotropy terms now included, we next calculate numerically the total effective field at each spin site, which is the functional derivative of the energy with respect to that spin. A new configuration is then chosen by aligning the spins with the total effective field at each site. The procedure is repeated until convergence is reached. Using this equilibrium configuration a Green’s function method is applied to investigate the SW excitations. Briefly, when the Hamiltonian is expanded in terms of boson operators, the linear term  $H^{(1)}$  vanishes with respect to the local axes and the quadratic term  $H^{(2)}$  can be diagonalized using a generalized Bogoliubov transformation. Details can be found elsewhere.<sup>14,15</sup>

To model a nanowire of 35-nm diam we choose the effective lattice constant  $a = 1.75$  nm, implying that the number  $N$  of spins in each layer equals 316 and 331 for the square and triangular lattices, respectively. Note that the value of  $a$  is well below the exchange length, which is of order 3–4 nm for permalloy. The magnetization and the exchange stiffness parameters, as well as the gyromagnetic ratio, of  $\text{Ni}_{80}\text{Fe}_{20}$  nanowires are those previously deduced in Ref. 10, namely  $M_s = 0.0645$  T,  $D = 9.30$  T nm<sup>2</sup>, and  $g\mu_B = 29.4$  GHz/T, and are not adjusted here. As noted before, they differ in some cases from those of bulk permalloy and were obtained by fitting the experimental data with the macroscopic theory of Ref. 13. The effective values of the exchange constant  $J$  and the spin  $S$  are related to  $M_s$  and  $D$  as shown in Ref. 14. The value of  $J_{\perp}$  is taken to be  $J$  for the square lattice, and  $2J/3$  for the triangular lattice. In the BLS experiments the component of the SW wave vector along the  $y$  direction is  $k = 0.040$  nm<sup>-1</sup>. Our calculations show that this finite value of  $k$ , although small compared to  $1/a$ , must be properly taken into account due to the dipole-dipole interactions.

Before discussing the role of anisotropy in this permalloy nanowire system, it is useful to compare the experimental results for the two different cases of longitudinal and transverse fields. The data points in Fig. 3 show that the dependence of the SW frequencies on the longitudinal applied magnetic field is, for the most part, linear. The frequency of the lowest SW mode is extrapolated to be  $\sim 9.8$  GHz at zero field. In contrast, the corresponding transverse magnetic field

$H_{\perp}$  dependence is far more complicated. Except for  $H_{\perp} = 0.33$  T, two magnon peaks were observed for transverse fields below 0.6 T (see Fig. 2). An unresolved peak was observed at  $H_{\perp} = 0.33$  T. Peculiarly, the frequency of the lowest-energy SW mode was measured to be 3.5 GHz at zero field and monotonically increases to 9.9 GHz at  $H_{\perp} = 0.6$  T where its intensity became very small. For transverse fields in the 0.6–1.2 T range, the lower-energy SW could not be detected, while the other mode could still be observed with a frequency that is strongly dependent on the magnetic field.

We are led to interpret the appearance of the new mode in the transverse case as an effect of single-ion anisotropy, since otherwise we find the SW behavior is qualitatively similar to that for nickel. Also, this anisotropy should presumably be very small and of the “easy-plane” type, because its presence was not evident in the longitudinal-field studies. By contrast, when the applied field is transverse, the spins are canted away from the symmetry axes and the magnetization becomes nonuniform. The anisotropy might then significantly add to the inhomogeneity of the magnetization and lead to the formation of a potential well for the SWs, which results in a spatially localized SW mode. The effects of SW potential well formation have been observed experimentally elsewhere in larger patterned elements of permalloy.<sup>5,6,12</sup> Those systems, however, are of micrometer size and nonellipsoidal in shape, and so therefore have a large shape anisotropy.

Based on the above observations, we systematically studied the role of single-ion anisotropy on the SW frequencies. We first carried out calculations for the longitudinal field case with the anisotropy set equal to zero and the magnetization assumed to be uniform and directed along the wire axis. The results are represented in Fig. 3 as the solid lines and, as might be expected, they are in very good agreement with the experimental data. This is due, in part, to the fact that the parameters used in the calculations, especially the exchange stiffness  $D$ , were those deduced by fitting the experimental data with the equivalent macroscopic theory, as mentioned earlier. If a small anisotropy is then added, the results are slightly different, implying a minor adjustment to the assumed value of  $D$  (or  $M_s$ ).

We next study the transverse case allowing for the presence of single-ion anisotropy and (for simplicity) keeping the other parameters unchanged. With the anisotropy coefficient  $K_n$  in Eq. (1) chosen to be  $K_{\text{surf}}$  at any surface site and  $K_{\text{bulk}}$  elsewhere, we carried out numerical calculations for the SW frequencies, concluding that the data are well reproduced only by taking  $K_{\text{surf}} < K_{\text{bulk}} < 0$ . The best overall fit was obtained with the anisotropies (in field units) given by  $H_{\text{surf}} \equiv SK_{\text{surf}}/g\mu_B = -0.15$  T and  $H_{\text{bulk}} \equiv SK_{\text{bulk}}/g\mu_B = -0.02$  T. These are the values assumed for the theory (solid lines) in Fig. 2; variations by  $\pm 0.05$  T for  $H_{\text{surf}}$  and  $\pm 0.01$  T for  $H_{\text{bulk}}$  lead to a noticeably inferior fit. The results presented here are for a square lattice forming the nanowire cross section. Similar calculations were carried out with the choice of a triangular lattice and we obtained very similar results, but with the anisotropies  $H_{\text{surf}}$  and  $H_{\text{bulk}}$  equal to  $-0.09$  and  $-0.01$  T, respectively, with the same range of uncertainties as quoted above. From consideration of the spatial distribution of SW amplitudes, we conclude that the second lowest branch in the theory for the transverse case (i.e., the solid line at  $\sim 7$  GHz

for small  $H_{\perp}$  in Fig. 2) behaves approximately as the uniform mode. Therefore it is expected to be unimportant for BLS studies.

In conclusion, we have reported BLS measurements for the quantized SWs in permalloy nanowires, showing that the modes and their dependence on applied magnetic field are quite distinct from the results for nickel. Further, we have successfully interpreted these data in terms of a microscopic theory that included inhomogeneous magnetization and an “easy-plane” surface anisotropy. From a device point of

view, this and the earlier study of nickel nanowires<sup>8</sup> show that surface effects can be very important in determining the energy of the lowest SW excitations in a ferromagnetic nanowire system. Thus it is important to consider not only the nanomagnetic material but also the role of surface anisotropy, which (together with the surface inhomogeneous magnetization<sup>18</sup>) contributes to the pinning. Further studies directed toward the physical origin of this surface anisotropy would be of interest.

\*Author to whom correspondence should be addressed. Email address: cottam@uwo.ca

<sup>1</sup>J. G. Zhu, Y. Zheng, and G. A. Prinz, *J. Appl. Phys.* **87**, 6668 (2000).

<sup>2</sup>*The Physics of Ultra-High-Density Magnetic Recording*, edited by M. L. Plumer, J. van Ek, and D. Weller (Springer, Berlin, 2001).

<sup>3</sup>*Spin Dynamics in Confined Magnetic Structures I*, edited by B. Hillebrands and K. Ounadjela (Springer, Berlin, 2002).

<sup>4</sup>S. O. Demokritov, B. Hillebrands, and A. N. Slavin, *Phys. Rep.* **348**, 441 (2001).

<sup>5</sup>J. Jorzick, S. O. Demokritov, B. Hillebrands, M. Bailleul, C. Fermion, K. Y. Guslienko, A. N. Slavin, D. V. Berkov, and N. L. Gorn, *Phys. Rev. Lett.* **88**, 047204 (2002).

<sup>6</sup>C. Bayer, S. O. Demokritov, B. Hillebrands, and A. N. Slavin, *Appl. Phys. Lett.* **82**, 607 (2003).

<sup>7</sup>C. Bayer, J. Jorzick, B. Hillebrands, S. O. Demokritov, R. Kouba, R. Bozinoski, A. N. Slavin, K. Y. Guslienko, D. V. Berkov, N. L. Gorn, and M. P. Kostylev, *Phys. Rev. B* **72**, 064427 (2005).

<sup>8</sup>Z. K. Wang, M. H. Kuok, S. C. Ng, D. J. Lockwood, M. G. Cottam, K. Nielsch, R. B. Wehrspohn, and U. Gösele, *Phys. Rev. Lett.* **89**, 027201 (2002).

<sup>9</sup>Z. K. Wang, H. S. Lim, H. Y. Liu, S. C. Ng, M. H. Kuok, L. L. Tay, D. J. Lockwood, M. G. Cottam, K. L. Hobbs, P. R. Larson, J. C. Keay, G. D. Lian, and M. B. Johnson, *Phys. Rev. Lett.* **94**, 137208 (2005).

<sup>10</sup>H. Y. Liu, Z. K. Wang, H. S. Lim, S. C. Ng, M. H. Kuok, D. J. Lockwood, M. G. Cottam, K. Nielsch, and U. Gösele, *J. Appl. Phys.* **98**, 046103 (2005).

<sup>11</sup>M. Demand, A. Encinas-Oropesa, S. Kenane, U. Ebels, I. Huynen, and L. Piraux, *J. Magn. Magn. Mater.* **249**, 228 (2002).

<sup>12</sup>J. P. Park, P. Eames, D. M. Engebretson, J. Berezovsky, and P. A. Crowell, *Phys. Rev. Lett.* **89**, 277201 (2002).

<sup>13</sup>R. Arias and D. L. Mills, *Phys. Rev. B* **63**, 134439 (2001).

<sup>14</sup>T. M. Nguyen and M. G. Cottam, *Phys. Rev. B* **71**, 094406 (2005).

<sup>15</sup>T. M. Nguyen and M. G. Cottam, *Phys. Rev. B* **72**, 224415 (2005).

<sup>16</sup>E. V. Tartakovskaya, *Phys. Rev. B* **71**, 180404(R) (2005).

<sup>17</sup>K. Nielsch, F. Müller, A. P. Li, and U. Gösele, *Adv. Mater. (Weinheim, Ger.)* **12**, 582 (2000).

<sup>18</sup>K. Y. Guslienko and A. N. Slavin, *Phys. Rev. B* **72**, 014463 (2005).